Journal of Polymer Research (2021) 28:191
https://doi.org/10.1007/s10965-021-02490-5

ORIGINAL PAPER

Water sorption behavior of phenol formaldehyde resin reinforcing with reduced graphene oxide and ZnO decorated graphene oxide

Sandhya P. K[1] · M. S. Sreekala[2] · Moothetty Padmanabhan[1,3] · Sabu Thomas[1]

Received: 5 August 2020 / Accepted: 8 March 2021

Abstract

The effect of two different fillers such as (a) reduced graphene oxide (RGO) produced by the reduction of graphene oxide (GO) using potato starch and (b) zinc oxide decorated graphene oxide (ZnO-RGO) on the water transport properties of phenol formaldehyde (PF) nanocomposites have been investigated at different temperatures. The effect of filler content, nature of filler and temperature on the water sorption of the PF nanocomposites were also studied. The results showed that the RGO content facilitates water uptake while ZnO-RGO filler impedes the water sorption properties of various nanocomposites developed. The diffusion, sorption and permeability coefficient of PF nanocomposites with varying weight percentage of filler at different temperatures were determined. The effect of temperature on the water sorption of PF nanocomposites was studied by determining the activation energy using Arrhenius equation. The thermodynamic studies revealed that the water sorption was spontaneous due to the negative value of ΔG^{o} and the reaction was exothermic because of the negative value of ΔH. The kinetic studies showed that the water sorption of the PF nanocomposites follows a first order reaction.

Keywords Phenol formaldehyde · Water sorption · Reduced graphene oxide · ZnO-RGO

Introduction

Phenolic resins are known for their diverse applications in various fields such as automobile, aerospace, and thermal insulation materials due to their excellent chemical resistance, thermal and mechanical properties. It is possible to tune and enhance their properties by addition of appropriate nanomaterials even in trace quantity by forming their nanocomposites. However, for their wide practical applications it is essential to understand the performance of these materials in various environmental situations including high humidity, supernormal temperature and even conditions when the materials are submerged or immersed in water, in which case the water uptake capacity or the material can be a matter of concern or interest depending upon the situation. In such a context, the study of sorption, diffusion and water permeation properties of the polymer nanocomposites are of great interest, especially for their more efficient and long-term applications in engineering, industry and even in ambient conditions. Graphene is considered as one of the most widely used two-dimensional materials for the preparation of polymer nanocomposites. Graphene related materials can be prepared from naturally abundant and inexpensive graphite, but the synthetic realization of pure graphene is indeed

Highlights
- Two new series of phenol formaldehyde (PF) nanocomposites are developed with RGO and ZnO-RGO as nanofillers by solution mixing followed by compression moulding
- Water sorption properties of the nanocomposites are studied at different temperatures
- The diffusion, sorption and permeability coefficient associated with water sorption by the PF nanocomposites are evaluated
- The effect of temperature on water sorption of the nanocomposites is studied by Arrhenius equation
- Thermodynamic and kinetic aspects of water sorption by the nanocomposites are studied

✉ M. S. Sreekala
sreekalams@yahoo.co.in

[1] School of Chemical Sciences, Mahatma Gandhi University, Kerala, Kottayam 686560, India

[2] Post Graduate Research Department of Chemistry, Sree Sankara College, Kerala, Kalady 683574, India

[3] Department of Chemistry, Amrita Vishwa Vidyapeetham, Kerala, Amritapuri 690525, India

Published online: 28 April 2021

very challenging and expensive [1]. In contrast, graphene oxide (GO), a two-dimensional carbon sheet and an oxidative derivative of graphene, has become a highly acceptable and environment-friendly substitute for graphene due to its non- toxicity, low cost of the precursor material and relative ease of preparation [1, 2]. The production of these single-layered carbon sheet-like material, almost akin to graphene sheets, in bulk quantity is possible by the reduction of GO through various routes. One important feature of these reduced graphene oxides (RGO) is the presence of diverse functional groups such as hydroxyl, epoxy, carbonyl, and carboxylate moieties in them which can facilitate and enhance interfacial bonding between the polymer matrix and RGO sheets through hydrogen bonding, π-π stacking, electrostatic forces and van der Waals interactions [3, 4]. These functional groups can also facilitate the homogeneous dispersion of RGO in the polymer matrix and improve the properties of the polymer matrix.

Generally, more studies in water sorption were conducted in the field of fiber reinforced polymer matrices. Sisal fiber, kenaf fiber, banana fiber and rice husk hybrids are separately used with thermosetting polymer shows better results in water sorption properties [5]. Hydrophilicity and structural arrangement of fibers within the polymer are the important factors that affect water sorption. Water sorption studies based on glass microsphere/epoxy composite [6] oil palm fiber reinforced and glass fiber reinforced PF composites [7], sisal fibre reinforced PF composites [8] short banana fiber-reinforced polyester composite materials [9] were also reported in many publications. The presence of lignocelluloses in natural fibers made them hydrophilic in nature and increases the water sorption of the polymer composites. The water transport studies on nanoclay based polymer such as epoxy, polyamide, polyester, polylactide were reported elsewhere [10–13]. The water sorption studies based on metal oxide (aluminium oxide) reinforced polymer nanocomposites is also reported [14].

There are several factors which can affect the molecular transport through a polymer matrix such as the nature of fillers, type of the material, cross-link density of the polymer used, the interaction between matrix and fillers, size and shape of the penetrant, aggregation of the filler, temperature etc. [15]. The diffusion processes also get affected by the nature of the solvent and its interaction with thermoset polymers such as phenol formaldehyde, epoxy resin, polyurethane, etc. The water transport studies on various nanoclay based polymer system such as epoxy, polyamide, polyester, polylactide were reported elsewhere [10–13]. The water sorption studies based on metal oxide (aluminium oxide) reinforced polymer nanocomposites is also reported [14]. Usually, the graphene sheets and the highly cross-linked nature of the polymer matrix lead to the formation of the tortuous path and hence decrease the sorption ability of the polymer nanocomposites. The nature of functional groups on the surface of graphene sheets can also affect the sorption property of polymer nanocomposites. For example, any hydrophilic or polar groups available on the filler material like RGO which are dispersed in the polymer matrix would enhance the water sorption ability of the polymer nanocomposites. In the case of graphene reinforced polymer nanocomposites, the aggregation of graphene sheets may produce new pathways for the diffusion of water molecules [16].

The nature and extent of water sorption in a polymer system are mostly governed by free volume of the polymer (which depend on the cross link density of the polymer) and also the affinity and local mobility of water molecules within the polymer matrix which depend on the formation of H-bonding or other electrostatic interaction between the matrix and polar water molecules [17]. The three mechanisms involved in water transport are (a) the presence of micro-voids or micro-cracks that are already present in the material or which get formed as a result of the interaction with water molecules, (b) sorption by both matrix and fillers through direct contact with water molecules and (c) a mode in which the interface between the filler and matrix act as a pathway for the diffusion of water molecules [6].The diffusion behavior of polymers based on relative mobilities of the polymer and penetrant is governed by (a) Fickian behavior, in which the rate of diffusion is smaller than the relaxation modes of polymer matrix (b) Non-Fickian pathway in which the diffusion process is faster than the relaxation process of the polymer matrix, and (c) anomalous behavior in which diffusion and relaxation rates are comparable and the micro-voids that are present in the polymer influencing the sorption and transport properties of the molecules. The water molecules which enter into the polymer matrix can reside in micro-voids as free water or it can interact with the polar groups present in the polymer matrix [18]. As a convenient and rapid method, gravimetric methods are used for evaluating and estimating the interactions between polymer and solvent.

The studies on the water sorption of PF based graphene nanocomposites have not been reported so far. The water transport property of epoxy/MWCNT composites was studied by Starkova and colleagues [17]. They found that the absorbed water has a strong influence on the diffusion and plasticization effects on the matrix. As a result of water absorption, the nanocomposites showed a decrease in storage modulus than that of neat epoxy. Yousefi and co-workers prepared polyurethane/graphene nanocomposites and studied the moisture permeability [19]. They reported that the moisture permeability of nanocomposites decreases with increasing the weight percentage of graphene and attributed such a behavior to the moisture barrier property, the horizontal alignment, and the very high aspect ratio of graphene sheets they used. Damari and colleagues studied the influence of lateral size and concentration of graphene on the water vapor permeability and mechanical

properties of polyurethane [20]. They observed that the degree of exfoliation and rheological percolation threshold are the factors which contribute to the water vapor permeation and mechanical performance of the nanocomposites.

The favourable exfoliation of single or multiple graphene nanosheets from raw graphite sheets limited by the intermolecular π-π stacking attraction forces and van der Waals interactions between graphene sheets [21]. The nature of interfacial interactions/bonding between graphene nanosheets and polymer matrix also plays a major role in modifying the properties of nanofillers, polymer matrix and, hence, the final nanocomposites. The dispersion of GO in natural rubber (NR) matrix was improved, increased the curing regions of rubber gum, provide the rubber entanglement that created the tortuous path to reduce the solvent diffusion. The permeation which occurs through pores, pinholes or microscopic cracks present in the polymer is called the Pore effect or Knudsen flux and is inversely proportional to the square root of the molecular weight of the permeant [22]. Charoenchai et al. fabricated hybrid silica-graphene oxide (SiO2@GO) nanocomposites by sol–gel method and introduced into NR matrix [23]. The swelling behavior of these nanocomposites was studied in toluene and their results showed that the aggregation of GO gets inhibited by SiO_2 nanoparticles on the GO surface.

The characterization of nanofillers, mechanical, thermal, viscoelastic and electrical properties of the PF/RGO and PF/ZnO-RGO nanocomposites were studied by various groups [24–28]. Thermogravimetric studies showed that PF nanocomposites are thermally stable up to 300 °C after which they undergo major decomposition processes [25, 27]. The thermal stability of the nanocomposites was seen to be affected by the nature and dispersion of the fillers and also based on filler-PF matrix interactions. The thermal properties of the nanocomposites experienced barrier effect and promoter effect, the barrier effect of the nanofillers enhance the thermal stability of the nanocomposites while the promoter effect would accelerate the degradation process of the matrix thereby decreasing their thermal stability. X-ray diffraction studies were used to analyze the crystalline behavior of the nanofillers and the nanocomposites. RGO reinforced nanocomposites are free of any crystalline peaks whereas ZnO-RGO filled nanocomposites at higher wt% shows crystallinity, mainly due to the aggregation of highly crystalline ZnO-RGO [25, 27]. The investigations related to the effect of crystallinity on water vapor transport in polymer nanocomposites becomes more difficult due to the nucleating agent behavior of the nanoparticles and its presence affects the crystalline morphology of polymers [10].

The present study involves the preparation of two categories of polymer nanocomposites viz., PF/RGO and PF/ZnO-RGO and investigation on their water sorption properties. The RGO we have developed is through a novel and a green route, in which we have used abundantly available potato starch as a reductant to reduce the graphene oxide (GO). Further, we could prepare ZnO decorated RGO (ZnO-RGO) and use the same for developing PF/ZnO-RGO nanocomposites [24, 25]. We have used two different types of nanofillers for our study because the water affinity of RGO and ZnO are widely different and therefore it is possible to modulate water sorption ability of their PF composites by judicious choice of their combinations. Further, we have monitored the effect of temperature on the water sorption ability of the PF-nanocomposites developed. The variations seen in the sorption properties of the different PF nanocomposites could be explained based on the morphology and chemical properties of both nanofillers and PF matrix. The diffusion coefficient, sorption coefficient, permeability coefficient and the kinetic parameters associated with the water sorption could be evaluated and the results explained. The thermal and kinetic behaviors of the sorption properties of the nanocomposites were also investigated and analyzed the results.

Experimental

Materials

Phenol formaldehyde resole resin is used as the matrix material and is obtained from Polyformalin, Kochi, Kerala, India. The chemicals used for the synthesis of nanofillers are graphite powder, potassium permanganate ($KMnO_4$), sodium nitrate ($NaNO_3$), ammonia, N,N-dimethylformamide (DMF), concentrated sulphuric acid (conc. H_2SO_4), hydrogen peroxide (H_2O_2), zinc acetate dihydrate ($Zn(CH_3COO)_2.2H_2O$) were purchased from Merck, India. Potato starch was procured from (LOBA Chemie Pvt. Ltd).

Preparation of nanofillers

Natural graphite powder was the starting material for the preparation of nanofillers RGO and ZnO-RGO. Graphite is converted into GO by Hummer's method [29]. RGO is obtained by reducing GO using eco-friendly reducing agent potato starch by refluxing at 80 ºC for 3 h. ZnO-RGO is synthesized by refluxing GO with zinc acetate dihydrate at 95 ºC for 5 h. The detailed methods of preparation of nanofillers and their characterization were reported in our previous study [24].

Preparation of PF nanocomposites

The PF nanocomposites with varying wt% of nanofiller (RGO and ZnO-RGO) were prepared by compression molding the semi-cured samples at 100 °C for 30 min, which is obtained

after mechanical mixing and sonication for 1 h at 60 ℃ of the nanofillers. The detailed method of preparation of nanocomposites and its characterization was discussed in our research article published elsewhere [25]. The cooled samples were cut in the desired shape and used for water sorption studies.

Characterization techniques

One of the important factors that affect the water sorption of the PF nanocomposites is the morphology of the nanofillers. The Scanning Electron Microscope (JEOL JSM -820 model) and Transmission Electron Microscope (JEM-2100HRTEM) images were used for studying the morphology of the nanofillers. XPERT-PRO X-ray diffractometer using Ni-filtered Cu with Kα radiation (θ = 1.5406 Å) and an operating voltage of 45 kV and a filament current of 35 mA is used for measuring the XRD of samples.

Water sorption studies of nanocomposites

Rectangular samples of 10 × 10 mm^2 size were cut from the nanocomposite sheet and the corners of the samples were made curved to avoid the non-uniform water transport [7]. The thickness and weight of the samples are measured before it is immersed in water in the diffusion bottles at different temperatures (30 °C, 50 °C, and 70 °C). The samples were taken out from the diffusion bottles in regular intervals of time and the excess water molecules adhered to the surface of the samples was wiped off gently and weighed in a precise balance and continued till equilibrium is reached.

Results and discussion

Water sorption studies of PF/RGO and PF/ZnO-RGO nanocomposites

In the case of polymers, the transport of small molecules follows solution diffusion kinetics. In other words, the polymer first absorbed the penetrant molecules followed by diffusion through the polymer. The mol % uptake of the solvent (Q_t) for the samples was determined using the equation given below [30, 31]

$$Q_t \,\text{mol}\,\% = \frac{(W_2 - W_1)/M_s}{W_1} \times 100 \tag{1}$$

where W_1 and W_2 are the weights of the specimen before and after swelling, and M_s is the molar mass of the solvent. The Q_t mol % uptake for each composite was calculated and plotted against the square root of time ($\sqrt{t}$.)

The SEM and TEM images of RGO and ZnO-RGO sheets are shown in Fig. 1a–d. From Fig. 1a large number of graphene sheets can be observed. In the case of ZnO-RGO, it can be seen that on the two-dimensional sheet-like the structure of graphene large number of ZnO nanoparticles are thickly spread on them. The ZnO nanoparticles are very closely packed and make the surface denser (Fig. 1b). It can also be observed that as a result of the growth of ZnO nanoparticles on the surface of the graphene sheet, the nanoparticles are strongly bound to its surface. The sheet-like structure of graphene is observed from the TEM image of RGO (Fig. 1c)

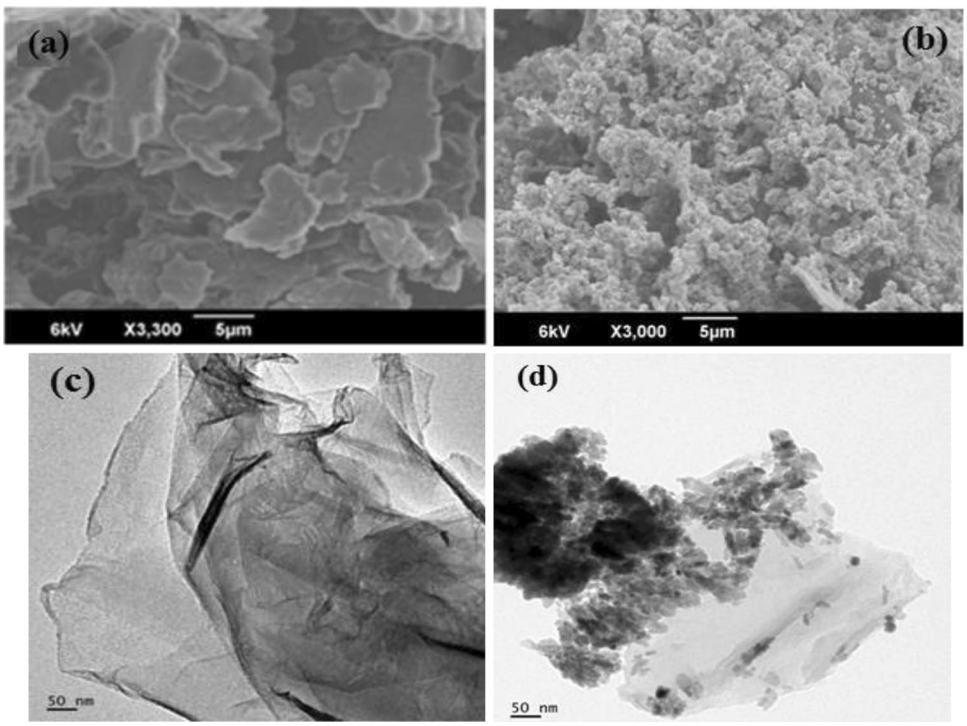

Fig. 1 SEM image of **(a)** RGO **(b)** ZnO-RGO and TEM image of **(c)** RGO **(d)** ZnO-RGO

[25]. The ZnO nanoparticles are decorated on the surface of GO sheets are observed from the TEM image of ZnO-RGO (Fig. 1d) [25].

The XRD curves of PF nanocomposites with RGO and ZnO-RGO nanofillers are as shown in Fig. 2a, b. The XRD peaks (Fig. 2a) of RGO filled nanocomposites and neat PF are same indicating the reinforcement of RGO into the PF matrix and good interfacial interaction with the matrix [25]. In the case of ZnO-RGO (Fig. 2b), the XRD curves at lower wt% and neat PF are similar. But at higher wt% the characteristic peak of ZnO-RGO at $2\theta = 36.48°$ (Fig. 2c) is observed and confirms that the high amount of ZnO-RGO affects the dispersion of nanofiller in the matrix [27]. The present manuscript is mainly focus on the water sorption behavior of PF nanocomposites at three different temperatures. The different characterizations of the nanofillers and the TEM images of the PF nanocomposites were reported in our previous works published elsewhere [25, 27].

Figure 3a–c represents the mol% uptake of PF/RGO nanocomposites with varying weight percentages of RGO at 30 °C. From the given figures, it is clear that the mol% uptake of the PF/RGO nanocomposites increases with an increase in RGO content. Neat PF (0% RGO) is a three-dimensionally cross-linked structure and practically no sorption of water occurs. Here, the sorption may be due to the presence of micro-cracks present in the neat PF [32]. In the case of nanocomposites, the sorption may be due to the presence of abundant hydrophilic nature of potato starch attached on the surface of graphene oxide as a result of the reduction of graphene oxide. With an increase in RGO content, the aggregation of RGO sheets occurs in the PF matrix and leading to a new tortuous path in the nanocomposite for the passage of water molecules. In the case of all samples, the mol% uptake increases first and reaches an equilibrium state. The microscopic interactions of water molecules with cross-linked polymer chains may lead to the swelling and physical relaxations of polymer chains. The swelled polymer chain increased the elasticity of the chain, which further increases the chemical potential and restricts the further absorption of water molecules and an equilibrium stage is attained. The increase in the water sorption of nanocomposites can be explained by several factors. At lower wt % of RGO, there was good interaction between PF and RGO and the hydroxyl groups available for interaction with water molecules are less. So at lower wt % RGO, the water sorption is low. But, at higher wt % RGO, the interaction

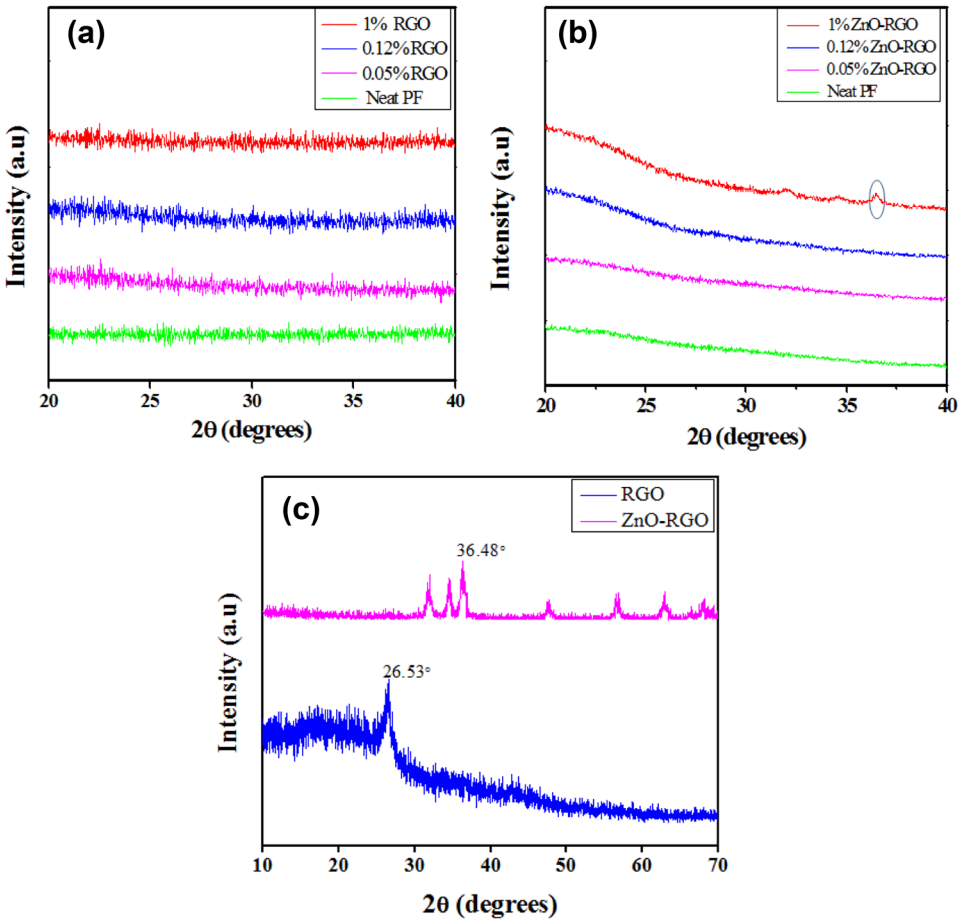

Fig. 2 XRD of **(a)** PF/RGO and **(b)** PF/ZnO-RGO nanocomposites **(c)** RGO and ZnO-RGO

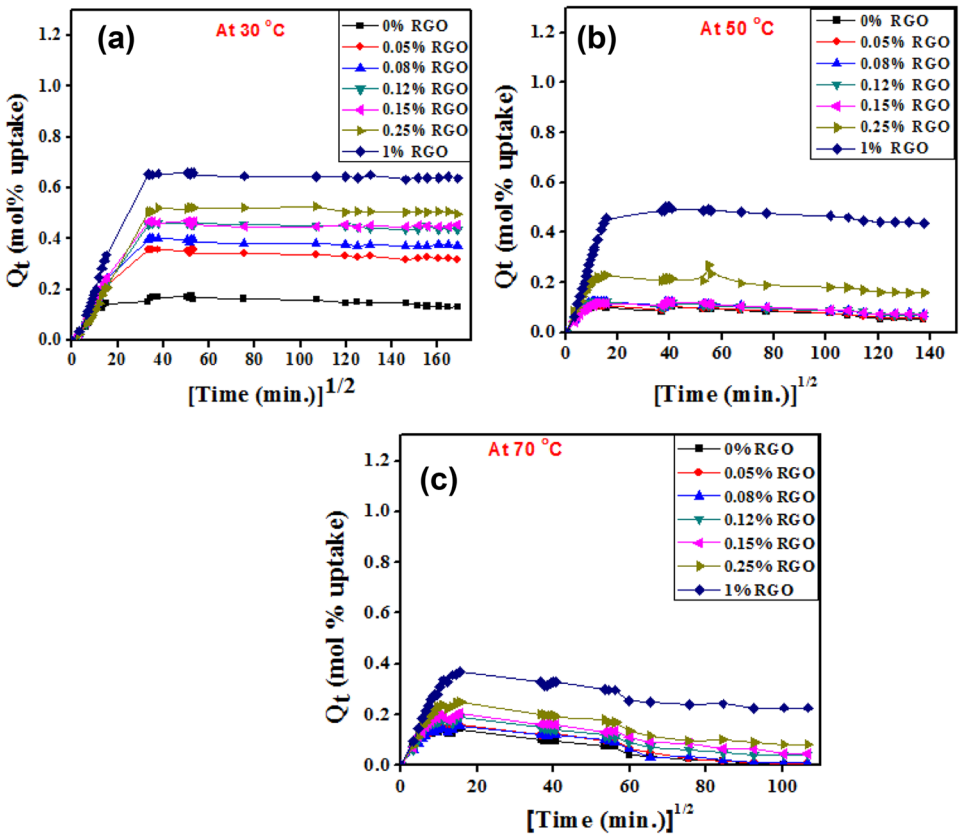

Fig. 3 Water uptake of PF/RGO nanocomposites at **(a)** 30 °C **(b)** 50 °C and **(c)** 70 °C

between PF and RGO are less and more number of hydroxyl groups from potato starch are available for hydrogen bonding interaction with water molecules. Moreover, at higher wt% RGO leads to the aggregation of RGO sheets which introduce the new pathways for the diffusion of water molecules [16]. The presence of abundant hydrophilic groups on the surface of graphene sheets and the availability of free volume are responsible for the diffusion of water molecules throughout the polymer matrix. Figure 3b, c illustrates the water sorption of PF/RGO nanocomposites at 50 °C and 70 °C with different RGO content. From the figures, it is clear that mol% uptake decreases with an increase in wt% RGO. In the case of neat PF and PF/RGO nanocomposites, the increase in temperature decreases the diffusion of water molecules.

In the case of nano reinforced polymers, a large number of polar groups are produced during the curing process and these are responsible for interaction and forming hydrogen bonds with water molecules. The presence of graphene sheets also alters the polymer chain packing. Figure 4a–c shows the mol% uptake of water at 30 °C, 50 °C and 70 °C. In the case of ZnO decorated graphene oxide, the presence of polar groups available for forming hydrogen bonds with water is less as compared with RGO obtained by starch potato reduction. Thus, the mol% uptake of ZnO-RGO filled nanocomposites shows a decreasing trend as compared to RGO filled nanocomposites.

In the case of ZnO decorated graphene oxide the presence of polar groups available for forming H-bonds with water is less as compared with RGO obtained by reduction using potato starch. As a result, the mol% uptake of water at 50 °C decreases with an increase in wt% of ZnO-RGO as compared to water sorption at 30 °C. Moreover, with the increase in wt% of filler, the free volume present in the polymer matrix decreased and it is occupied by the filler. This also leads to a decrease in mol% uptake of water with an increase in wt% of ZnO-RGO. But at 70 °C, the PF/ZnO-RGO nanocomposites show an increase in mol% uptake of water as compared to other temperatures. In other words, the high temperature affects the diffusion of water molecules through PF nanocomposites.

In our study, the chemical modification on GO sheets is a factor that determines the water uptake of PF nanocomposites. The ZnO decorated graphene oxide nanocomposites show water sorption behavior lower than that of neat PF. When we decorate GO using ZnO, GO was reduced to graphene oxide and at the same time ZnO changes to nano ZnO. These nanoparticles increase the surface area available for interaction with the graphene sheets and matrix, thus reducing the water uptake of PF/ZnO-RGO nanocomposites. Since three-dimensionally cross-linked PF is a hydrophobic material, it can prevent the entry of water molecules, the PF nanocomposites exhibit the lowest water uptake. On

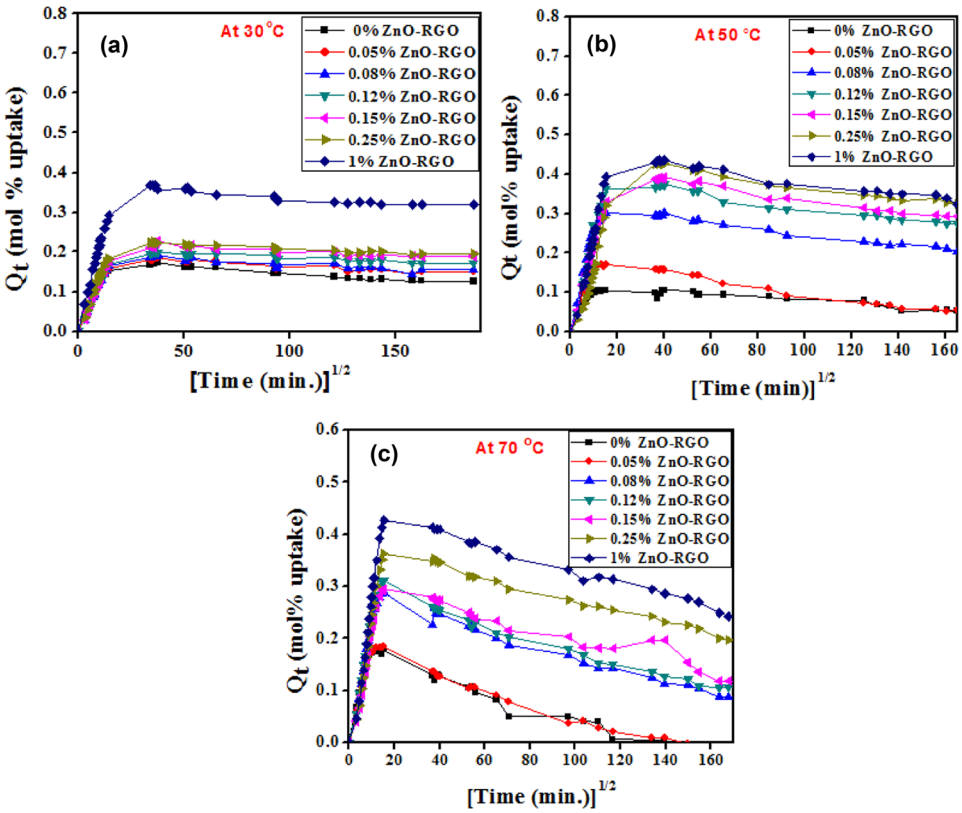

Fig. 4 Water uptake of PF/ZnO-RGO nanocomposites at **(a)** 30 **(b)** 50 and **(c)** 70 °C

examining the water uptake curves all the samples show an initial increase due to the rapid absorption of water molecules and reach a saturation point after that there was no increase in absorption of water molecules. In other words, the content of water molecules on the nanocomposites remains the same. An interesting feature observed at 70 °C is that the water uptake increases with an increase in wt% of ZnO-RGO. Here, the minimum water uptake is observed for neat PF and the maximum is for nanocomposites with1 wt% of ZnO-RGO. A schematic representation of water transport occurred in PF/RGO and PF/ZnO-RGO nanocomposites are shown in Fig. 5.

Diffusion, sorption and permeability coefficient of PF/RGO and PF/ZnO-RGO nanocomposites

The diffusion, sorption and permeability coefficients are considered as the important parameters that determine the effectiveness of the diffusion process. The diffusion coefficient depends on the segmental mobility of the polymer. It gives information about the rate at which the diffusion process occurs. It is a kinetic parameter and is defined as the rate of transfer of the diffusing substance across the unit area of cross-section divided by the space gradient of concentration.

Diffusion coefficient (D) can be calculated by the following equation [33]

$$D = \pi \left(\frac{h\theta}{4Q_\infty} \right)^2 \tag{2}$$

where h represents the initial thickness of the sample, θ is the slope of the initial linear portion of the sorption curve. The slope is calculated from Q_t versus $\sqrt{t}$. Q_∞ is the mol % uptake at equilibrium.

The sorption coefficient (S) depends on the strength of interactions present in the polymer and the penetrant molecule. It is a thermodynamic parameter and gives the measurement of extend of sorption. Sorption also gives information about the initial penetration and dispersal of water molecules into the polymer matrix. Sorption coefficient [34] is calculated by

$$S = M_\infty / M_0 \tag{3}$$

where M_∞ is the mass of water taken up at equilibrium and M_0 is the initial mass of the polymer sample.

The permeability coefficient (P) [35] gives information about the water permeated through the uniform area of the sample per second. Generally, permeation through any matrix is a combination of diffusivity as well as the sorption of the penetrant in the polymer. It is expressed as the product of diffusion and sorption coefficients.

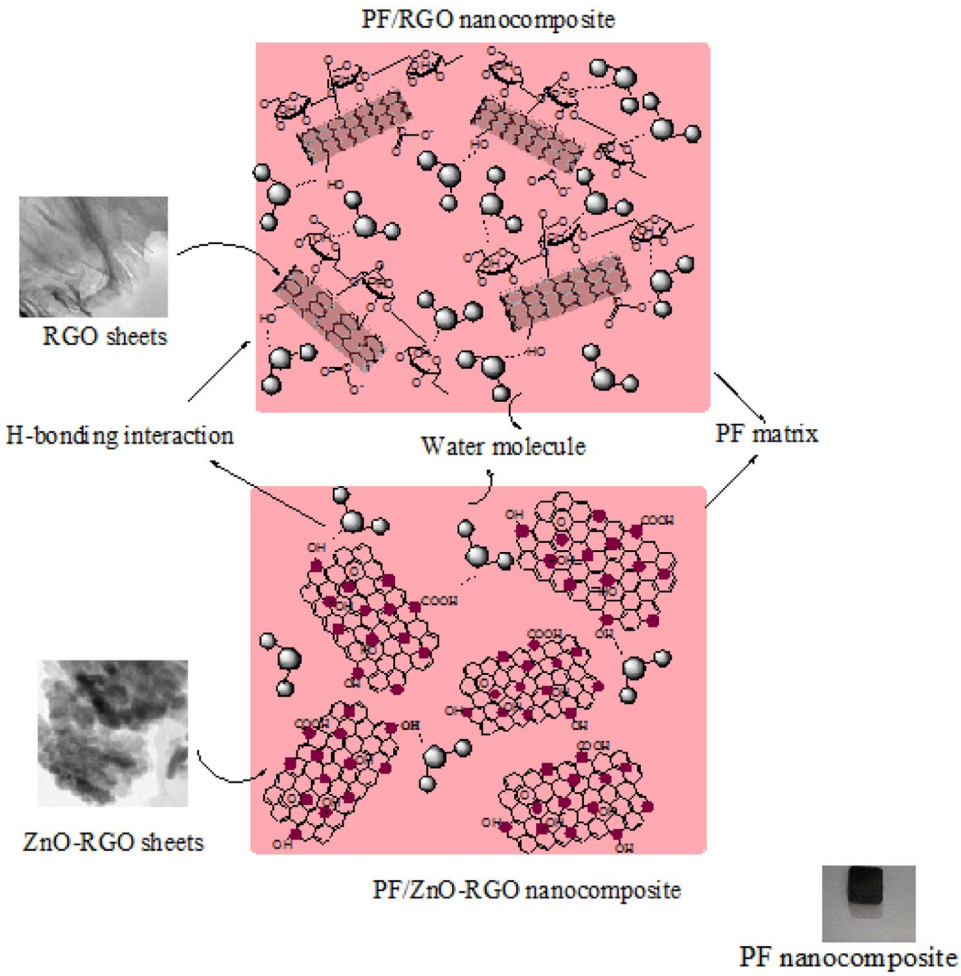

Fig. 5 Schematic representation of water transport in PF/RGO and PF/ZnO-RGO nanocomposites

$$P = D \times S \tag{4}$$

The diffusion coefficient (D), sorption coefficient (S) and permeability coefficient (P) of PF/RGO nanocomposites are calculated using the equations from 2 to 4 and the obtained values at different temperatures are furnished in Table 1.

The concentration of the available space for accommodating the penetrant molecule is an important factor that affects the diffusion process. When the penetrant molecule acquires sufficient energy it can jump to the neighboring hole. The diffusion coefficient is a measure of the ability of water molecules to move into the PF matrix. The decrease in water diffusion coefficient was also due to the clustering of water molecules in a hydrophobic material [16]. The diffusion coefficient is independent of nanocomposites loadings because it measures the flow of water in one dimension along with the thickness of the sample [36].

The penetration of water molecules through the polymer matrix also depends on the sorption coefficient and it is a direct indicator of absorbed solvent in the polymer. From the Table 1, it is clear that with the increase in wt% RGO there is a slight change in the sorption coefficient is observed. At three different temperatures, the maximum value of the sorption coefficient is observed for nanocomposites with 1 wt% RGO. It is also noted that the value of the sorption coefficient is close to one in all PF nanocomposites at three different temperatures. From this, it is clear that temperature and RGO content produces very little change in the sorption properties of PF/RGO nanocomposites.

The permeability coefficient gives a combined effect of diffusion and sorption coefficients. The permeability coefficient decreases with an increase in wt % RGO at 30 °C, 50 °C and 70 °C. With an increase in temperature, the permeation coefficient increases. With the increase in RGO content, there is a decrease in permeability is observed for PF/RGO nanocomposites.

The calculated values of diffusion, sorption and permeability coefficient of PF/ZnO-RGO nanocomposites were tabulated in Table 2. From the table, it is observed that at 30 °C, 50 °C, and 70 °C, D value of PF/ZnO-RGO nanocomposites decreased with an increase in temperature. At higher filler loading, the free volume available for the transport of water molecules decreases. Moreover, the average path length required for the transport of water molecules

Table.1 Diffusion coefficient (D), sorption coefficient (S) and permeability coefficient (P) of PF/ RGO nanocomposites having varying RGO content at different temperatures

RGO content (wt %)	D (cm^2s^{-1})	S	P (cm^2s^{-1})
At 30 °C			
0	1.9910×10^{-6}	1.0226	2.0360×10^{-6}
0.05	2.7995×10^{-7}	1.0571	2.9595×10^{-7}
0.08	3.2845×10^{-7}	1.0672	3.5051×10^{-7}
0.12	3.9549×10^{-7}	1.0776	4.2619×10^{-7}
0.15	3.8920×10^{-7}	1.0817	4.2099×10^{-7}
0.25	4.1691×10^{-7}	1.0894	4.5418×10^{-7}
1	4.2054×10^{-7}	1.1147	4.6878×10^{-7}
At 50 °C			
0	1.1714×10^{-5}	1.0094	1.1824×10^{-5}
0.05	1.2379×10^{-5}	1.0099	1.2502×10^{-5}
0.08	2.8393×10^{-6}	1.0365	2.9431×10^{-6}
0.12	2.2197×10^{-6}	1.0495	2.3297×10^{-6}
0.15	1.4697×10^{-6}	1.0528	1.5472×10^{-6}
0.25	1.8788×10^{-6}	1.0583	1.9884×10^{-6}
1	1.9112×10^{-6}	1.0583	2.0227×10^{-6}
At 70 °C			
0	1.4686×10^{-3}	1.0003	1.4691×10^{-3}
0.05	1.9115×10^{-4}	1.0013	1.9140×10^{-4}
0.08	1.3039×10^{-4}	1.0017	1.3062×10^{-4}
0.12	2.6313×10^{-5}	1.0077	2.6517×10^{-5}
0.15	1.7123×10^{-5}	1.005	1.7208×10^{-5}
0.25	1.5199×10^{-5}	1.0125	1.5389×10^{-5}
1	1.0616×10^{-5}	1.0361	1.0999×10^{-5}

Table.2. Diffusion coefficient (D), sorption coefficient (S) and permeability coefficient (P) of PF/ZnO-RGO nanocomposites having varying ZnO-RGO content at different temperatures

Zn)-RGO content (wt %)	D (cm^2s^{-1})	S	P (cm^2s^{-1})
At 30 °C			
0	1.9910×10^{-6}	1.0226	2.0360×10^{-6}
0.05	1.8934×10^{-6}	1.0272	1.9450×10^{-6}
0.08	1.8706×10^{-6}	1.028	1.9231×10^{-6}
0.12	1.8234×10^{-6}	1.0309	1.8798×10^{-6}
0.15	1.5120×10^{-6}	1.034	1.5635×10^{-6}
0.25	1.3244×10^{-6}	1.035	1.3708×10^{-6}
1	1.1505×10^{-6}	1.0573	1.2164×10^{-6}
At 50 °C			
0	1.1714×10^{-5}	1.0094	1.1824×10^{-5}
0.05	1.2379×10^{-5}	1.011	1.1691×10^{-5}
0.08	2.8393×10^{-6}	1.0131	1.0440×10^{-5}
0.12	2.2197×10^{-6}	1.0125	1.0301×10^{-5}
0.15	1.4697×10^{-6}	1.0131	1.0189×10^{-5}
0.25	1.8788×10^{-6}	1.0291	3.3973×10^{-6}
1	1.9112×10^{-6}	1.0796	2.8809×10^{-6}
At 70 °C			
0	1.4686×10^{-3}	1.0003	1.4691×10^{-3}
0.05	2.6596×10^{-4}	1.0018	2.6643×10^{-4}
0.08	1.7798×10^{-5}	1.0139	1.8046×10^{-5}
0.12	1.5580×10^{-5}	1.0133	1.5788×10^{-5}
0.15	1.1741×10^{-5}	1.0179	1.1951×10^{-5}
0.25	3.0929×10^{-6}	1.0336	3.1969×10^{-6}
1	3.0825×10^{-6}	1.0442	3.2186×10^{-6}

increases and lead to a decrease in diffusion coefficient [37]. With the increase in temperature, the diffusion coefficient of PF/ZnO-RGO nanocomposites increases. This may be due to the fact that an increase in temperature leads to a decrease in the interaction energy.

The sorption coefficients (S) of PF/ZnO-RGO nanocomposites increase with an increase in wt% of ZnO-RGO at three different temperatures. In almost all cases, with an increase in temperature, there is a decrease in sorption coefficients of nanocomposites is observed. It is also observed that the sorption values are close to one in varying ZnO-RGO contents and at different temperatures, indicating that the filler and temperature can produce a very small change in sorption properties. The permeability coefficient (P) of PF/ZnO-RGO nanocomposites decreases with increase in wt% of ZnO-RGO and increases with an increase in temperature.

Mechanism of water transport

The empirical relation used for analyzing the results of sorption experiments is given by [38],

$$\log\frac{Q_t}{Q_\infty} = \log K + n\log t \tag{5}$$

where Q_t is the mol% uptake at time t and Q_∞ is the mol% sorption at equilibrium. The term K is a constant characteristic of the polymer, indicates the interaction between the polymer and water. An idea of the mechanism of sorption is given by the value of n. When the value of n = 0.5, the diffusion obeys Fick's law and the mechanism of sorption is said to be Fickian [39]. It occurs when the segmental mobility of the polymer chains is faster than the rate of diffusion of the permeant molecules. When the value of n = 1, the mechanism of sorption obeys non-Fickian. This happens when the rate of diffusion of permeant molecules is much less than the segmental mobility of the polymer chains. If the value of n is between 0.5 and 1 the diffusion is said to be anomalous.

Table 3 represents the n and K values of PF/RGO nanocomposites at 30 °C, 50 °C, and 70 °C. From the table, it is clear that the values of n at 30 °C are around 0.6 suggesting that the transport mechanism shows a deviation from the normal Fickian behavior. At 50 °C

Table 3 n and K values of PF/RGO nanocomposites having varying RGO content at different temperatures

RGO content (wt %)	Temperature (°C)	n	K (min^{-1})
0	30	0.594	0.071
	50	0.444	0.296
	70	0.317	6.654
0.05	30	0.737	0.016
	50	0.612	0.187
	70	0.413	3.233
0.08	30	0.668	0.016
	50	0.422	0.102
	70	0.422	2.361
0.12	30	0.634	0.013
	50	0.417	0.036
	70	0.498	0.468
0.15	30	0.667	0.012
	50	0.439	0.05
	70	0.483	0.515
0.25	30	0.658	0.013
	50	0.399	0.026
	70	0.521	0.268
1	30	0.548	0.015
	50	0.689	0.019
	70	0.548	0.118

Table 4 n and K values of PF/ZnO-RGO nanocomposites having varying ZnO-RGO content at different temperatures

ZnO-RGO content (wt %)	Temperature (°C)	n	K (min^{-1})
0	30	0.594	0.071
	50	0.444	0.296
	70	0.317	6.654
0.05	30	0.635	0.048
	50	0.426	0.295
	70	0.509	1.847
0.08	30	0.668	0.043
	50	0.422	0.263
	70	0.696	0.119
0.12	30	0.634	0.043
	50	0.417	0.295
	70	0.659	0.119
0.15	30	0.667	0.036
	50	0.439	0.221
	70	0.733	0.063
0.25	30	0.658	0.039
	50	0.399	0.209
	70	0.745	0.04
1	30	0.548	0.061
	50	0.689	0.031
	70	0.783	0.032

and 70 °C, the values n are less than 0.5 in most cases and it follows a less Fickian behavior. But at higher wt% (0.25 and 1), the values of n are close to 0.5 at 70 °C and the transport mechanism shows Fickian behavior. The magnitude of K value represents the interaction between the polymer and the solvent. At all temperatures, the K values of PF/RGO nanocomposites are lower than neat PF, which indicates the interaction between the PF chain and water molecules that can be reduced by the presence of RGO sheets.

The n and K values of PF/ZnO-RGO nanocomposites are tabulated in Table 4. From the table, it is clear that the values of n at 30 °C are around 0.6 suggesting that the transport mechanism shows a deviation from the normal Fickian behavior. At 50 °C, the n values of the nanocomposites are less than 0.5 indicating that nanocomposites show 'Less Fickian' behavior. But at 70 °C, above 0.08 wt% ZnO-RGO the n value is higher than 0.6 suggesting that the mechanism shows a deviation from the normal Fickian behavior. With the increase in wt% of ZnO-RGO, the n value of nanocomposites showed an irregular trend at all temperatures. The filled samples have lower K values than unfilled samples at 30 °C and 70 °C, but at 50 °C, an irregularity was observed throughout the samples.

Effect of temperature on the water sorption of PF/RGO nanocomposites

Diffusion and permeation are thermally activated processes. The temperature-dependent behavior can be used for calculating the activation energy of water sorption of PF/RGO nanocomposites. The activation energy of PF/RGO nanocomposites was determined using Arrhenius equation [40] from the water sorption studies at three different temperatures (30 °C, 50 °C, and 70 °C) is given by

$$X = X_0 e^{-E/RT} \tag{6}$$

where X is P or D, X_0 represents P_0 or D_0, which are constants, E is the activation energy, R is the universal gas constant, and T is the absolute temperature.

Figure 6a, b represents the plot of log D and log P versus 1/T of various PF/RGO nanocomposites. The values of activation energies of diffusion (E_D) and permeation (E_P) were estimated and the heat of sorption (ΔH_s) was obtained from the difference between E_P and E_D ($\Delta H_s = E_P — E_D$). The obtained values of E_D, E_P, and ΔH_s are compiled in Table 5. The value of E_D and E_P of nanocomposites decrease with an increase in wt% RGO, indicating that only little energy was needed for the diffusion and permeation of water through

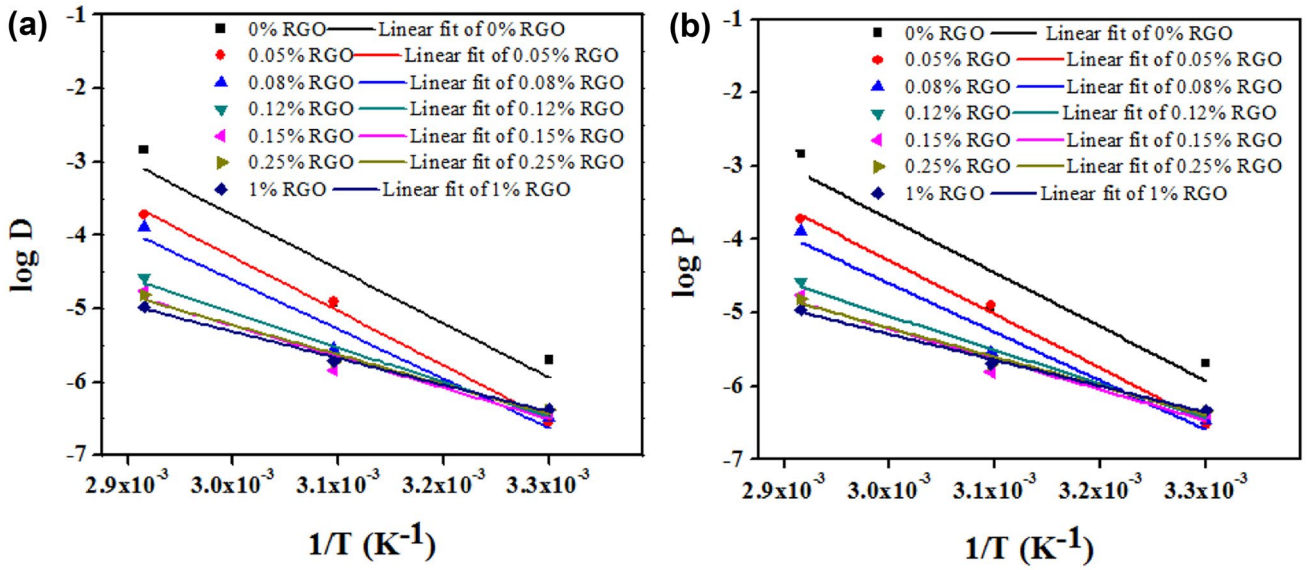

Fig. 6 **(a)** log D versus 1/T graph and **(b)** log P versus 1/T graph of PF/RGO nanocomposites

nanocomposites. The value of E_p decreases with the introduction RGO from 140.65 kJ/mol (0% RGO) to 47.30 kJ/mol (1wt% RGO). E_D value decreases from 141.13 kJ/mol to 47.71 kJ/mol. The value of ΔH_s gives information about the transport of water molecules through the polymer matrix. The energy needed to jump the dissolved molecules from one hole into another is termed as the activation energy of diffusion. Here, the values are found to be negative indicating that the sorption is mainly dominated by Langmuir's mode with a hole-filling mechanism that plays the main role in water sorption, giving an exothermic contribution to the sorption process.

The PF/ZnO-RGO nanocomposites showed resistance to water uptake at 30 °C and 50 °C. But at 70 °C, the water uptake of nanocomposites showed an increasing trend. The activation energy of PF/ZnO-RGO nanocomposites was determined using the Arrhenius equation. The plot of log D and log P versus 1/T of various PF/ZnO-RGO nanocomposites is given in Fig. 7a, b. The values of Arrhenius parameters E_D, E_P, and ΔH_s for water sorption in PF/ZnO-RGO nanocomposites were tabulated in Table 6. With the increase in wt% ZnO-RGO, the values of E_D and E_P of nanocomposites decrease up to 0.25 wt%, and an increase is observed for 1 wt%. The ΔH_s values are found to be negative for all composites, following the Langmuir's sorption mode. The ΔH_s value increase with an increase in wt% of ZnO-RGO. ΔH_s value for 0 wt% ZnO-RGO is -2.52 kJ/mol and for 1 wt % ZnO-RGO it is -0.3 kJ/mol.

Thermodynamics of water sorption of PF/RGO nanocomposites

The van't Hoff equation [40] used for the calculation of thermodynamic parameters such as ΔH^0 and ΔS^0 is as follows

$$\log K_s = \frac{\Delta S^0}{2.303R} - \frac{\Delta H^0}{2.303RT} \tag{7}$$

where K_s is the equilibrium sorption constant and is given by

$$K_s = \frac{No.\ of\ moles\ of\ solvent\ sorbed\ at\ equilibrium}{Mass\ of\ polymer} \tag{8}$$

R is the universal gas constant and T is the absolute temperature.

Table 5 Values of Arrhenius parameters E_D, E_P, and ΔH_s for water sorption of PF/RGO nanocomposites

kJ/mol	RGO content (%)						
	0	0.05	0.08	0.12	0.15	0.25	1
E_P	140.65	98.58	90.65	57.44	52.35	51.91	47.3
E_D	141.13	99.13	91.21	57.94	52.98	52.38	47.71
ΔH_s	-0.48	-0.55	-0.56	-0.5	-0.62	-0.47	-0.41

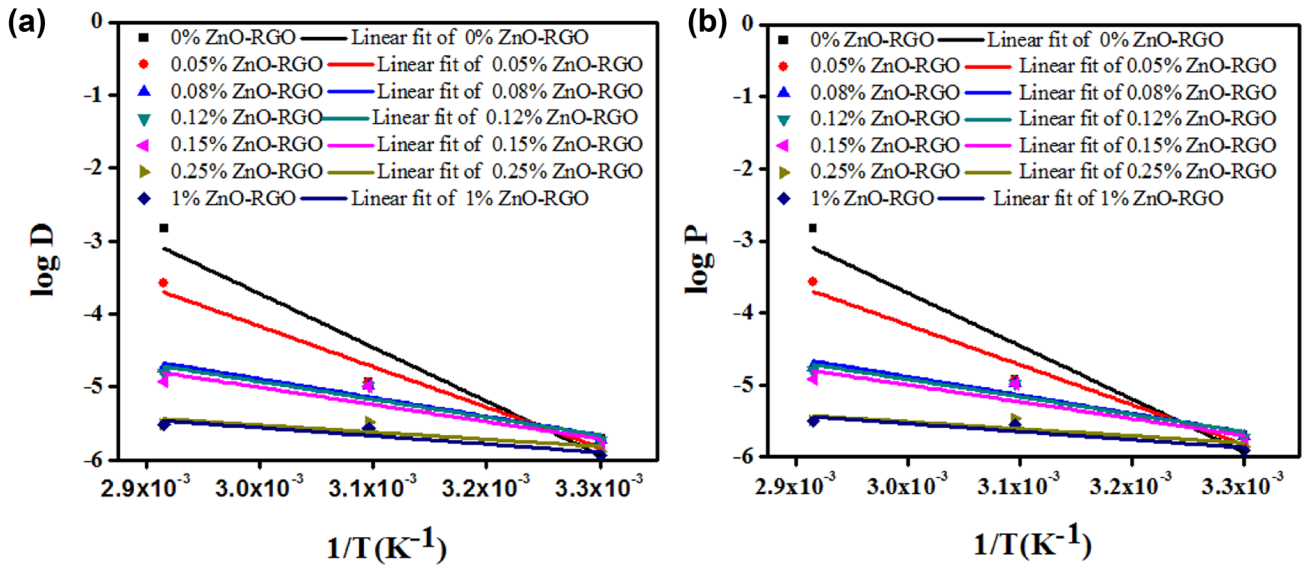

Fig. 7 **(a)** log D versus 1/T graph and **(b)** log P versus 1/T graph of PF/ZnO-RGO nanocomposites

The regression analysis plots of log K_s versus 1/T gives the values of ΔS^0 and ΔH^0. Figure 8 (a) represents the plot of log K_s versus 1/T. The free energy ΔG^0 can be calculated using the following equation

$$\Delta G^0 = \Delta H^0 - T\Delta S^0 \quad (9)$$

where T is the temperature in Kelvin.

The values of ΔH^0, ΔS^0, and ΔG^0 were tabulated in Table 7. The negative values of ΔH indicated that the sorption process is exothermic. The positive values of ΔS indicated the increase in randomness at the solid-solute interface when the adsorption process occurs. The feasibility of the process is confirmed by the negative value of Gibb's free energy. The negative value of ΔG also indicated the spontaneous nature of the process at all temperature ranges.

The thermodynamic parameters such as ΔH^0 and ΔS^0 of PF/ZnO-RGO nanocomposites were calculated using van't Hoff equation (Eq. 7). Table 8 represents the values of ΔH^0, ΔS^0, and ΔG^0 of PF/ZnO-RGO nanocomposites. From the table, it can be seen that all the samples have a negative ΔH^0 value indicating that the sorption process is exothermic in nature. ΔS^0 values are positive for all the samples. The negative value of ΔG^0 indicating the spontaneity of the sorption process and the values are found to be less negative with an increase in wt% of ZnO-RGO. Figure 8b represents the log K_s versus 1/T graph of PF/ZnO-RGO nanocomposites with varying wt% of ZnO-RGO.

Kinetics of water sorption of PF/RGO nanocomposites

The sorption in polymeric materials developed compressive stress and is controlled by the rate of polymer expansion. The transport of water through PF/RGO nanocomposites is a rate controlled kinetic process and can be studied by applying for first order kinetic rate equation as given below [7].

$$\frac{dC}{dt} = K'(C_\infty - C_t) \quad (10)$$

where K' is the first order rate constant, C_∞ and C_t are concentrations at time equilibrium and 't' respectively. The kinetic rate constant gives an idea about the speed at which

Table 6 Values of Arrhenius parameters E_D, E_P, and ΔH_s for water sorption of PF/ZnO-RGO nanocomposites

kJ/mol	ZnO-RGO content (%)						
	0	0.05	0.08	0.12	0.15	0.25	1
E_P	170.37	135.34	79.13	77.48	72.23	48.61	53.77
E_D	172.89	137.64	80.67	78.8	73.54	49.31	54.07
ΔH_s	-2.52	-2.3	-1.54	-1.32	-1.31	-0.7	-0.3

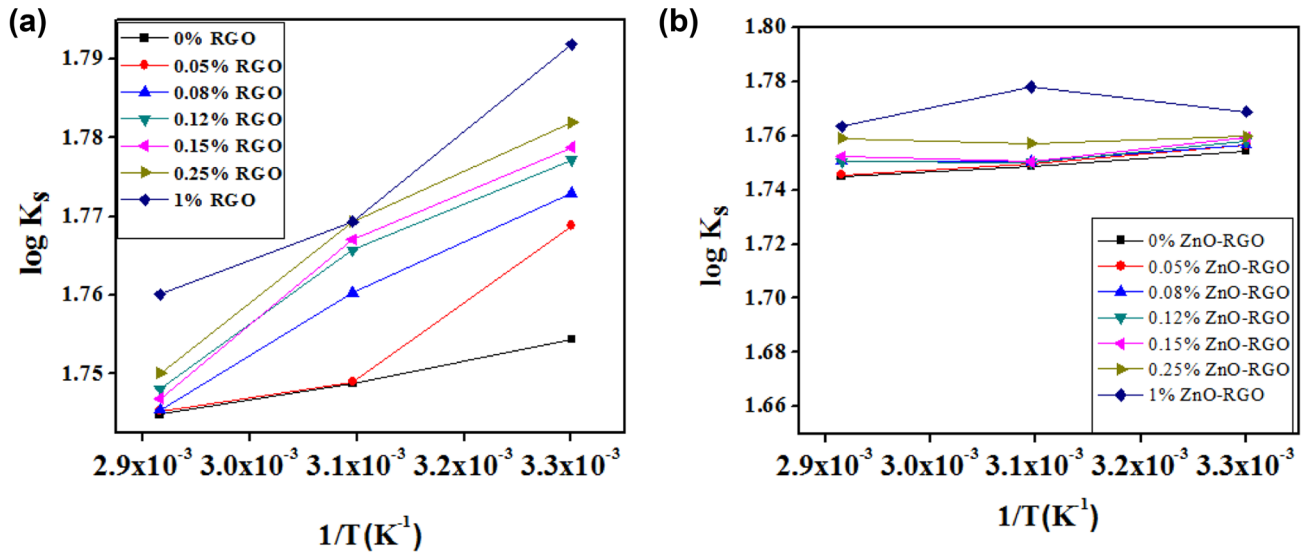

Fig. 8 log K_s versus 1/T graph of **(a)** PF/RGO and **(b)** PF/ZnO-RGO nanocomposites

Table 7 Thermodynamic parameters of PF/RGO nanocomposites

Sample (% RGO)	ΔH^0(kJ/mol)	ΔS^0(kJ/mol)	ΔG^0(kJ/mol)
0	-0.477	0.032	-10.017
0.05	-0.553	0.0318	-10.029
0.08	-0.562	0.0318	-10.032
0.12	-0.498	0.032	-10.034
0.15	-0.621	0.0316	-10.044
0.25	-0.47	0.0322	-10.053
1	-0.409	0.0326	-10.125

Table 8 Thermodynamic parameters of PF/ZnO-RGO nanocomposites

Sample (% RGO)	ΔH^0(kJ/mol)	ΔS^0(kJ/mol)	ΔG^0(kJ/mol)
0	-0.477	0.032	-10.017
0.05	-0.553	0.0318	-10.029
0.08	-0.562	0.0318	-10.032
0.12	-0.498	0.032	-10.034
0.15	-0.621	0.0316	-10.044
0.25	-0.47	0.0322	-10.053
1	-0.409	0.0326	-10.125

the water molecules penetrates through the medium [41]. On integration, the above equation can be written as

Table.9. Rate constants of PF nanocomposites

Sample	Rate Constant of PF/RGO ($\times 10^2$ min^{-1})	Rate Constant of PF/ZnO-RGO ($\times 10^2$ min^{-1})
0	3.14	3.14
0.05	4.52	1.69
0.08	4.32	1.75
0.12	3.43	1.31
0.15	4	1.15
0.25	2.74	1.31
1	3.9	1.14

$$\log\left(C_\infty - C_t\right) = \log C_\infty - \frac{K' t}{2.303} \tag{11}$$

On plotting '$\log\left(C_\infty - C_t\right)$' against 't' gives a straight line with a slope of -K'/2.303. The values of K' can be calculated from the slope and it can be compiled in Table 9. Figure 9a represents the plot of '$\log\left(C_\infty - C_t\right)$' versus time. The RGO reinforced systems showed lower rate constant values than neat PF. Figure 9b represents the log C_∞-C_t versus time graph. The rate constant of PF/ZnO-RGO nanocomposites with varying wt% of ZnO-RGO was tabulated in Table 9. The rate constant of nanocomposites is less than neat PF up to 0.25 wt% ZnO-RGO. From the Fig. 9a, b, it is clear that the nature of the plot is linear so that the water sorption of PF nanocomposites follows first order kinetics.

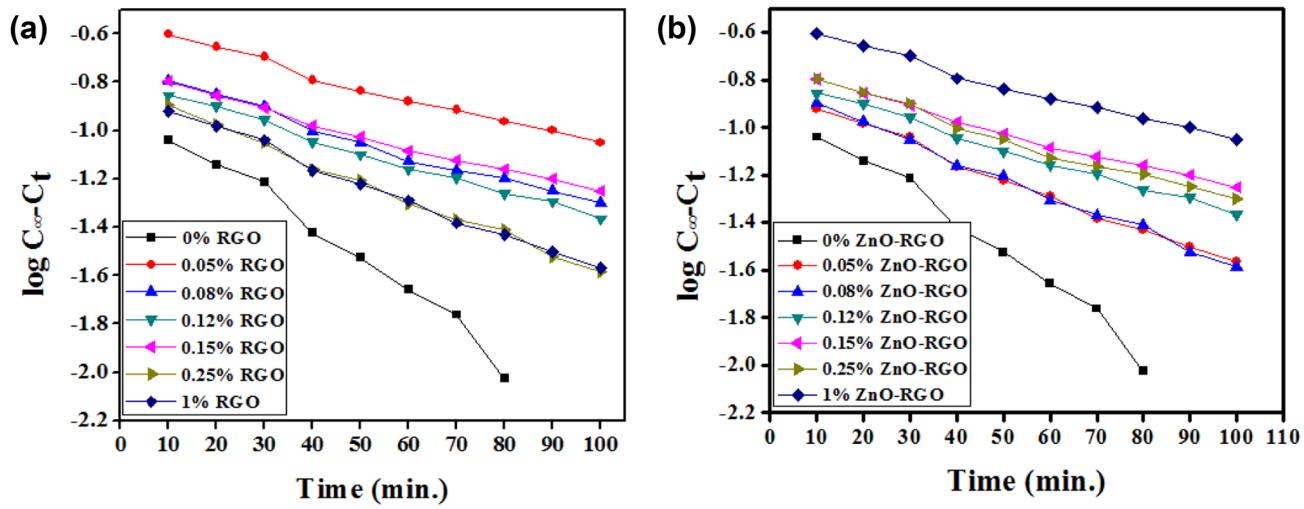

Fig. 9 Plot of '$\log\left(C_\infty - C_t\right)$' versus time of **(a)** PF/RGO **(b)** PF/ZnO-RGO nanocomposites

Conclusions

The effect of two different fillers RGO and ZnO decorated RGO (ZnO-RGO) on the water sorption of PF nanocomposites is investigated in three different temperatures such as 30 °C, 50 °C and 70 °C. From the results, it is observed that the water sorption of PF nanocomposites increased with an increase in the wt% of RGO. But with ZnO-RGO, the water sorption behavior of the PF nanocomposites decreases with an increase in wt% of ZnO-RGO. The difference in the sorption behavior may be explained on the basis of the morphology of the nanofiller, which is the chemical modification on the surface of graphene oxide (GO). The effect of temperature on the water sorption was studied by determining the activation energy using the Arrhenius equation. In the case of PF/RGO nanocomposites, the activation energy of permeation (from 140.65 kJ/mol to 47.30 kJ/mol) and diffusion (from 141.13 kJ/mol to 47.71 kJ/mol) decreases with increase in wt% of filler. But, in the case of PF/ZnO-RGO nanocomposites, the values of E_D and E_P of nanocomposites decreases up to 0.25 wt%, and an increase is observed for 1 wt%. The heat of sorption (ΔH_s) values is negative indicating an exothermic contribution to the sorption process in the case of both PF nanocomposites. From the thermodynamic studies, it is clear that the water sorption behavior of PF nanocomposites is spontaneous. The kinetic studies of the PF nanocomposites revealed that the water sorption follows first order kinetics.

Supplementary Information The online version contains supplementary material available at https://doi.org/10.1007/s10965-021-02490-5.

Acknowledgements The authors are grateful to the financial support under DST-FIST (No. 487/DST/FIST/15-16) New Delhi to Sree Sankara College, Kalady and Mahatma Gandhi University, Kottayam, India for the award of Junior Research Fellowship for Sandhya P K.

References

1. Bautkinová T, Sifton A, Kutorglo EM, et al (2020) New approach for the development of reduced graphene oxide/polyaniline nanocomposites via sacrificial surfactant-stabilized reduced graphene oxide. Colloids Surf A Physicochem Eng Asp 589. https://doi.org/10.1016/j.colsurfa.2020.124415
2. Aragaw BA (2020) Reduced graphene oxide-intercalated graphene oxide nano-hybrid for enhanced photoelectrochemical water reduction. J Nanostructure Chem 10:9–18. https://doi.org/10.1007/s40097-019-00324-x
3. Stankovich S, Dikin DA, Dommett GHB et al (2006) Graphene-based composite materials. Nature 442:282–286. https://doi.org/10.1038/nature04969
4. Li D, Müller MB, Gilje S et al (2008) Processable aqueous dispersions of graphene nanosheets. Nat Nanotechnol 3:101–105. https://doi.org/10.1038/nnano.2007.451
5. Badyankal PV, Manjunatha TS, Vaggar GB, Praveen KC (2020) Compression and water absorption behaviour of banana and sisal hybrid fiber polymer composites. Materials Today: Proceedings 8–11. https://doi.org/10.1016/j.matpr.2020.02.695
6. Lekatou A, Faidi SE, Ghidaoui D et al (1997) Effect of water and its activity on transport properties of glass/epoxy particulate composites. Compos A Appl Sci Manuf 28:223–236. https://doi.org/10.1016/S1359-835X(96)00113-3
7. Sreekala MS, Kumaran MG, Thomas S (2002) Water sorption in oil palm fiber reinforced phenol formaldehyde composites. Compos A: Appl Sci Manuf 33:763–777. https://doi.org/10.1016/S1359-835X(02)00032-5
8. Maya MG, George SC, Jose T et al (2017) Mechanical properties of short sisal fibre reinforced phenol formaldehyde eco-friendly composites. Polyme Renewable Res 8:27–42. https://doi.org/10.1177/204124791700800103

9. Sreekumar PA, Albert P, Unnikrishnan G et al (2008) Mechanical and water sorption studies of ecofriendly banana fiber-reinforced polyester composites fabricated by RTM. J Appl Polym Sci 109:1547–1555. https://doi.org/10.1002/app.28155
10. Trifol J, Plackett D, Szabo P, et al (2020) Effect of Crystallinity on Water Vapor Sorption, Diffusion, and Permeation of PLA-Based Nanocomposites. ACS Omega 0–7. https://doi.org/10.1021/acsomega.0c01468
11. Megahed AA, Agwa MA, Megahed M (2020) Can ultrasonic parameters affect the impact and water barrier properties of nanoclay filled glass fiber/polyester composites? J Ind Text. https://doi.org/10.1177/1528083720960733
12. Kouini B (2020) Water absorption and hygrothermal aging behaviors of polyamide66/maleated polypropylene/nanoclay nanocomposites. J Macromol Sci Part A Pure Appl Chem 57:512–518. https://doi.org/10.1080/10601325.2020.1733429
13. Chee SS, Jawaid M, Sultan MTH et al (2020) Effects of nanoclay on physical and dimensional stability of Bamboo/Kenaf/nanoclay reinforced epoxy hybrid nanocomposites. J Mater Res Technol 9:5871–5880. https://doi.org/10.1016/j.jmrt.2020.03.114
14. Nordell P, Nilsson F, Hedenqvist MS et al (2011) Water transport in aluminium oxide-poly(ethylene-co-butyl acrylate) nanocomposites. Eur Polymer J 47:2208–2215. https://doi.org/10.1016/j.eurpolymj.2011.09.013
15. Thomas S, Wilson R, Anil Kumar S, George SC (2017) Transport Properties of Polymeric Membranes
16. Tan B, Thomas NL (2016) A review of the water barrier properties of polymer/clay and polymer/graphene nanocomposites. J Membr Sci 514:595–612. https://doi.org/10.1016/j.memsci.2016.05.026
17. Starkova O, Buschhorn ST, Mannov E et al (2013) Water transport in epoxy/MWCNT composites. Eur Polymer J 49:2138–2148. https://doi.org/10.1016/J.EURPOLYMJ.2013.05.010
18. Becker O, Varley RJ, Simon GP (2004) Thermal stability and water uptake of high performance epoxy layered silicate nanocomposites. Eur Polymer J 40:187–195. https://doi.org/10.1016/J.EURPOLYMJ.2003.09.008
19. Yousefi N, Gudarzi MM, Zheng Q et al (2013) Highly aligned, ultralarge-size reduced graphene oxide/polyurethane nanocomposites: Mechanical properties and moisture permeability. Compos A Appl Sci Manuf 49:42–50. https://doi.org/10.1016/j.compositesa.2013.02.005
20. Peretz Damari S, Cullari L, Nadiv R et al (2018) Graphene-induced enhancement of water vapor barrier in polymer nanocomposites. Compos B Eng 134:218–224. https://doi.org/10.1016/j.compositesb.2017.09.056
21. Huang TM, Lin CK, Wu RJ, et al (2019) Development of segregated 3D graphene networks in rubber nanocomposites with enhanced electrical and mechanical properties. J Polym Res 26. https://doi.org/10.1007/s10965-019-1785-6
22. Prasad K, Nikzad M, Sbarski I (2018) Permeability control in polymeric systems: a review. J Polym Res 25. https://doi.org/10.1007/s10965-018-1636-x
23. Charoenchai M, Tangbunsuk S, Keawwattana W (2020) Silica-graphene oxide nanohybrids as reinforcing filler for natural rubber. J Polym Res 27. https://doi.org/10.1007/s10965-020-02209-y
24. Sandhya PK, Jose J, Sreekala MS et al (2018) Reduced graphene oxide and ZnO decorated graphene for biomedical applications. Ceram Int 44:15092–15098. https://doi.org/10.1016/j.ceramint.2018.05.143
25. Sandhya PK, Sreekala MS, Padmanabhan M et al (2019) Effect of starch reduced graphene oxide on thermal and mechanical properties of phenol formaldehyde resin nanocomposites. Compos B Eng 167:83–92. https://doi.org/10.1016/j.compositesb.2018.12.009
26. Sandhya PK, Sreekala MS, Xian G et al (2020) Viscoelastic and electrical properties of RGO reinforced phenol formaldehyde nanocomposites. J Appl Polym Sci 137:1–11. https://doi.org/10.1002/app.49211
27. Sandhya PK, Sreekala MS, Padmanabhan M, Thomas S (2020) Mechanical and thermal properties of ZnO anchored GO reinforced phenol formaldehyde resin. Diam Relat Mater 108:107961. https://doi.org/10.1016/j.diamond.2020.107961
28. Sandhya PK, Sreekala MS, Xian G et al (2020) Enhancement in electrical conductivity and dynamic mechanical properties of resole resin with ZnO-RGO as nanofiller. Diam Relat Mater 108:107934. https://doi.org/10.1016/j.diamond.2020.107934
29. Hummers WS, Offeman RE (1958) Preparation of Graphitic Oxide. J Am Chem Soc 80:1339–1339. https://doi.org/10.1021/ja01539a017
30. Mathew AP, Padmanabhan AS, Packirisamy S, Thomas S (1997) Kinetics of Diffusion of Styrene Monomer Containing Divinyl Benzene Through Vulcanized Natural Rubber. J Polym Eng 17:405–429. https://doi.org/10.1515/POLYENG.1997.17.5.405
31. Igwe IO (2007) Uptake of aromatic solvents by polyethylene films. J Appl Polym Sci 104:3849–3854. https://doi.org/10.1002/app.25980
32. Elwan I, Jabra R (2017) Preparation and evaluation of mechanical and physical properties of random silica fiber/modified resole resin composites. J Mater Environ Sci 8:1220–1234
33. Aminabhavi TM, Phayde HTS (1995) Molecular transport characteristics of Santoprene thermoplastic rubber in the presence of aliphatic alkanes over the temperature interval of 25 to 70°C. Polymer 36:1023–1033. https://doi.org/10.1016/0032-3861(95)93603-J
34. Ajithkumar S, Patel NK, Kansara SS (2000) Sorption and diffusion of organic solvents through interpenetrating polymer networks (IPNs) based on polyurethane and unsaturated polyester. Eur Polymer J 36:2387–2393. https://doi.org/10.1016/S0014-3057(00)00025-2
35. Chiou JS, Paul DR (1986) Sorption equilibria and kinetics of ethanol in miscible poly(vinylidene fluoride)/poly(methyl methacrylate) blends. Polym Eng Sci 26:1218–1227. https://doi.org/10.1002/pen.760261710
36. Alateyah AI, Dhakal HN, Zhang ZY (2014) Water Absorption Behavior, Mechanical and Thermal Properties of Vinyl Ester Matrix Nanocomposites Based on Layered Silicate. Polymer-Plastics Technol Eng 53:327–343. https://doi.org/10.1080/03602559.2013.844246
37. Abacha N, Kubouchi M, Sakai T (2009) Diffusion behavior of water in polyamide 6 organoclay nanocomposites. Express Polym Lett 3:245–255. https://doi.org/10.3144/expresspolymlett.2009.31
38. Moni G, Abraham J, Kurian C et al (2018) Effect of reduced graphene oxide on the solvent transport characteristics and sorption kinetics of fluoroelastomer nanocomposites. Phys Chem Chem Phys 20:17909–17917. https://doi.org/10.1039/c8cp02411a
39. Wang J, Wu W, Lin Z (2008) Kinetics and thermodynamics of the water sorption of 2-hydroxyethyl methacrylate/styrene copolymer hydrogels. J Appl Polym Sci 109:3018–3023. https://doi.org/10.1002/app.28403
40. Mathai AE, Thomas S (1996) Transport of aromatic hydrocarbons through crosslinked nitrile rubber membranes. J Macromol Sci, Phys 35:229–253. https://doi.org/10.1080/00222349608212383
41. Thomas N, Windle AH (1978) Transport of methanol in poly(methyl methacrylate). Polymer 19:255–265. https://doi.org/10.1016/0032-3861(78)90218-5